423 23. Gupta J, Grube E, Ericksen MB, Stevenson MD, Lucky AW, Sheth AP, et al.
424 Intrinsically defective skin barrier function in children with atopoic dermatitis
425 correlates with disease severity. J Allergy Clin Immunol 2008;121:725-30
426 24. Novac, N. New insights into the mechanism and management of allergic
427 diseases: atopic dermatitis. Allergy 2009;64:265-275
428 25. Kang JS, Lee K, Han SB, Ahn JM, Lee H, Han MH, et al. Induction of
429 atopic eczema/dermatitis syndrome-like skin lesions by repeated topical application
430 of a crude extract of *Dermatophagoides pteronyssinus* in NC/Nga mice. Int
431 Immunopharmacol 2006;6: 1616-1622
432 26. Yamamoto M, Haruna T, Yasui K, Takahashi H, Iduhara M, Takaki S, et al.
433 A Novel Atopic Dermatitis Model Induced by Topical Application with
434 *Dermatophagoides Farinae* Extract in NC/Nga Mice. Allergol Int. 2007;56:139-48
435 27. Matsumoto M, Ra C, Kawamoto K, Sato H, Itakura A, Sawada J, et al. IgE
436 hyperproduction through enhanced tyrosine phosphorylation of Janus Kinase 3 in
437 NC/Nga Mice, a model for human atopic dermatitis. J Immunol 1999;162:1056-
438 1063
439 28. Cooper D, Hales J, Camp R. IgE-dependent activation of T cells by allergen
440 in atopic dermatitis: Pathophysiologic relevance. J Invest Dermatol 2004;123:1086-
441 1091
442 29. Nemoto-Hasebe I, Akiyama M, Nomura T, Sandilands A, McLean WHI,
443 Shimizu H. Clinical severity correlates with impaired barrier in filaggrin-related
444 eczema. J Invest Dermatol 2009;129:682-689
445 30. Willis CM, Shaw S, Lacharriere OD, Baverel M, Reihe L, Jourdain R, et al.
446 Sensitive skin: an epidemiological study. Br J Dermatol 2001;145:258-263.
447 31. Farage MA, Katsarou A, Maibach HI. Sensory, clinical and physiological
448 factors in sensitive skin: a review. Contact Dermatitis 2006: 55: 1–14
449 32. Clayton TH, Wilkinson SM, Rawcliffe C, Pollock B, Clark SM. Allergic
450 contact dermatitis in children: should pattern of dermatitis determine referral? A

451 retrospective study of 500 children tested between 1995 and 2004 in one U.K.
452 centre. Br J Dermatol 2006;154:114-117
453 33. Mailhol C, Lauwers-Cances V, Rance F, Paul C, Giordano-Labadie F.
454 Prevalence and risk factors for allergic contact dermatitis to topical treatment in
455 atopic dermatitis: a study in 641 children. Allergy 2009;64:801-806
456 34. Yilmaz M, Bingöl G, Altintas D, Kendirli SG. Correlation between atopic
457 diseases and tuberculin responses. Allergy 2000;55:664-7
458 35. Grűber C, Kulig M, Bergmann R, Guggenmoos-Holzmann I, Wahn U,
459 MAS-90 Study Group. Delayed Hypersensitivity to Tuberculin, Total
460 Immunoglobulin E, Specific Sensitization, and Atopic Manifestation in
461 Longitudinally Followed Early Bacille Calmette-Guėrin-Vaccinated and
462 Nonvaccinated Children. Pediatrics 2001;107:e36
463 36. Kimura M, Tsuruta S, Yoshida T. Correlation of house dust mite-specific
464 lymphocyte proliferation with IL-5 production, eosinophilia, and the severity of
465 symptoms in infants with atopic dermatitis. J Allergy Clin Immunol 1998;101:85-89
466 37. Henderson J, Northstone K, Lee SP, Liao H, Zhao Y, Pembrey M, et al. The
467 burden of disease associated with filaggrin mutations: a population-based,
468 longitudinal birth cohort study. J Allergy Clin Immunol 2008;121:872-7
469 38. Vasilopoulos Y, Cork MJ, Teare D, Marinou I, Ward SJ, Duff GW, et al. A
470 nonsynonymous substitution of cystatin A, a cysteine protease inhibitor of house
471 dust mite protease, leads to decreased mRNA stability and shows a significant
472 association with atopic dermatitis. Allergy 2007;62:514-519
473 39. Jeong SK, Kim HJ, Youm JK, Ahn SK, Choi EH, Sohn MH, et al. Mite and
474 cockroach allergens activate protease-activated receptor 2 and delay epidermal
475 permeability barrier recovery. J Invest Dermatol 2008;128:1930-1939
476 40. Roeland T, Heughebaert C, Hachem JP. Proteolytically active allergens
477 cause barrier breakdown. J Invest Dermatol 2008;128:1878-1880
478
479
480

481 **Figure legend**

482 **Figure 1**. Spontaneous dermatitis of *ft/ft* mice in SPF. (A) Western blot analysis with anti-
483 filaggrin Ab. (B) The clinical pictures of 20-week-old *ft/ft* mice. (C,D) Total clinical
484 severity scores (C) with each particular item (D) of 5, 10 and 23-week-old *ft/ft* mice. (E)
485 HE-stained section in 8 and 18-week-old mice (bar=100μm). Toluidine blue staining of the
486 skin from 8-week-old B6 and *ft/ft* mice and the numbers of mast cells per field are shown
487 (F). $*P < 0.05$.
488
489 **Figure 2**. The skin barrier dysfunction in *ft/ft* mice. (A) TEWL on dorsal skin of 5, 8, and
490 16-week-old B6 and *ft/ft* mice. (B) The amount of FITC in the skin of B6 and *ft/ft* mice
491 after topical application. $*P<0.05$.
492
493 **Figure 3**. The immune status of the *ft/ft* mice in the steady state. (A) The total serum IgE
494 levels of B6 and *ft/ft* mice measured by ELISA. (B, C) The numbers of total cells (B), $CD4^+$,
495 and $CD8^+$ cells in the skin draining LN and spleen (C). $*P < 0.05$.
496
497 **Figure 4**. Enhanced cutaneous immune responses in *ft/ft* mice. The ear thickness change of
498 B6 and *ft/ft* mice after topical application of PMA for irritant contact dermatitis (A) and
499 DNFB challenge on the ears for CHS (B). (C) DTH response. B6 and *ft/ft* mice sensitized
500 with OVA intraperitoneally followed by elicitation on footpad subcutaneously. $*P < 0.05$.
501
502 **Figure 5**. Mite (Dp)-induced dermatitis model. B6 and *ft/ft* mice were topically applied of
503 ointment with (Dp) or without (Vas) Dp. (A-C) Clinical pictures after the last application of
504 Dp (A), clinical skin severity score (B), and ear thickness change (C) at each indicated time
505 points after application. (D, E) Histology of the skin (D), and the numbers of mast cells (E)
506 after the last application. Bar, 100 μm. (F) Scratching behavior. The number of scratching
507 (left) and the total duration of scratching (right) over 15 minutes after the last application.
508 (G) TEWL after the last application. (H) Serum mite-specific IgE levels. $*P < 0.05$.
509

Figure 1
Moniaga et al.

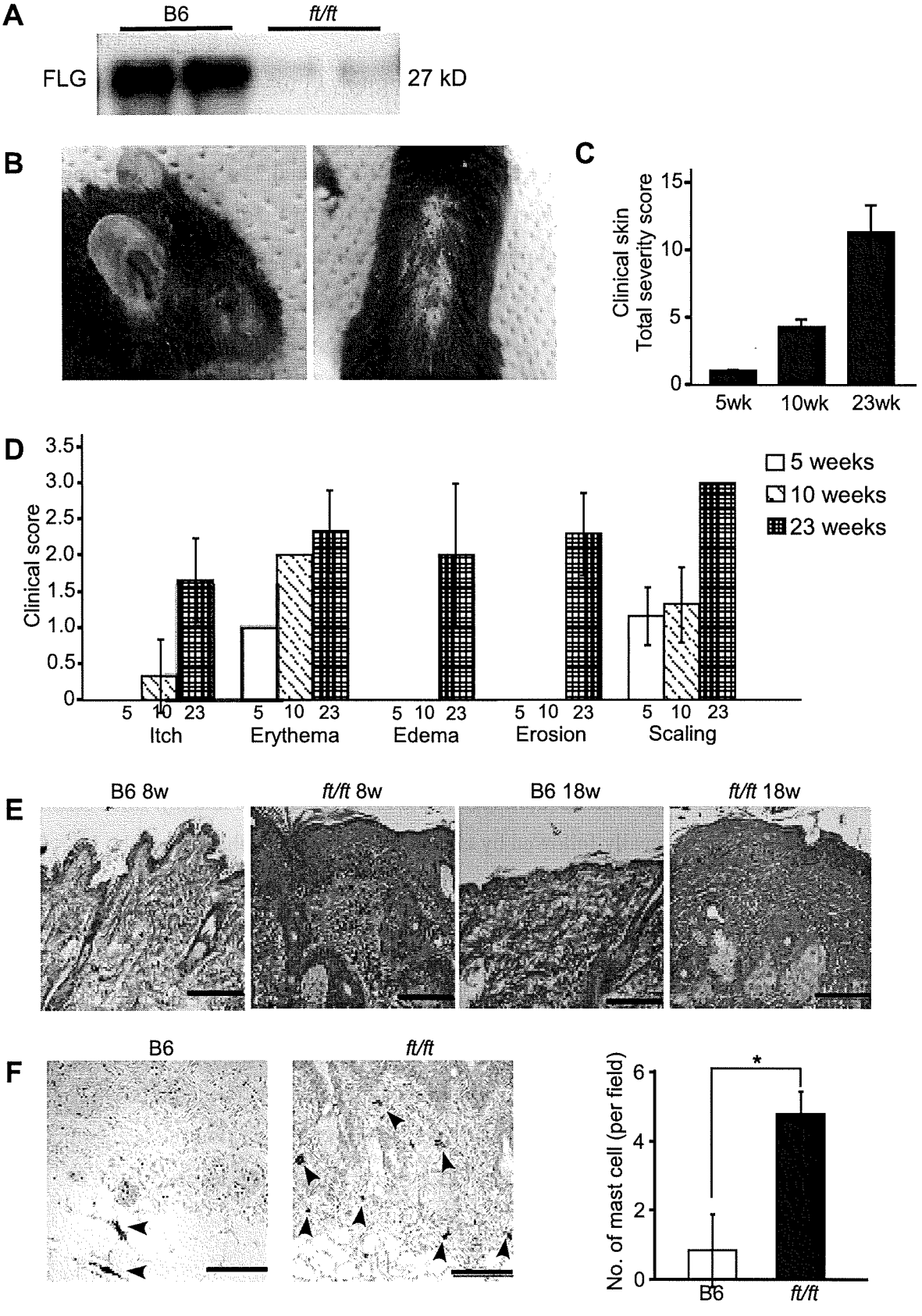

Figure 2
Moniaga et al.

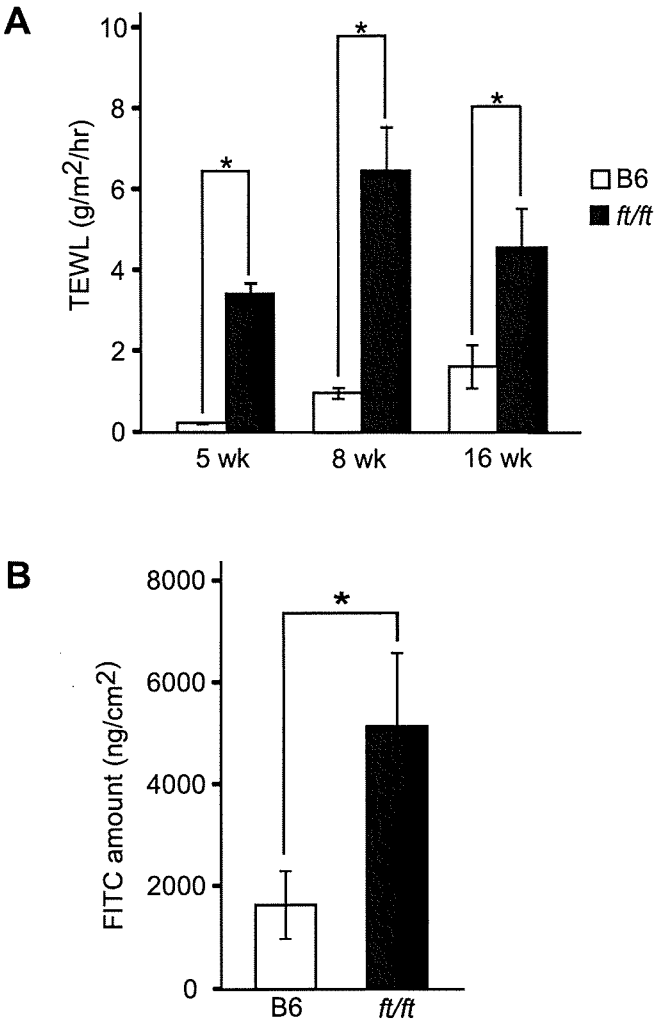

Figure 3
Moniaga et al.

A

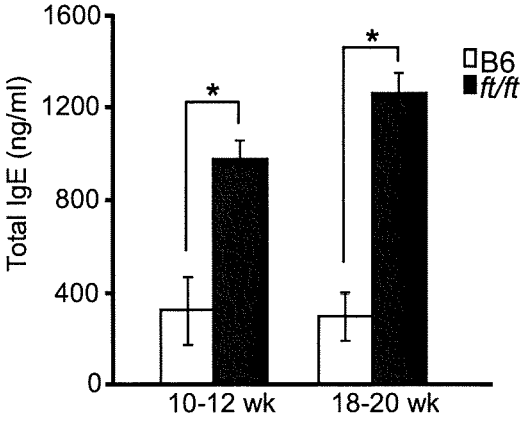

B

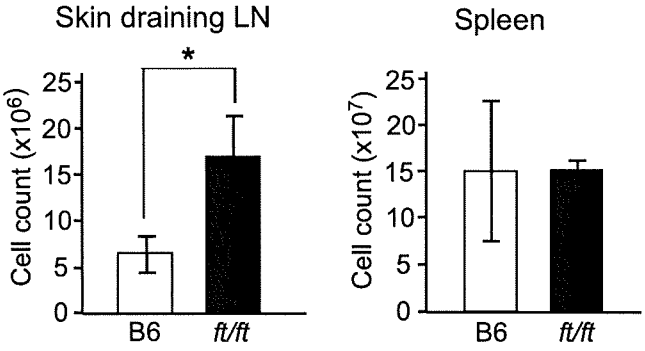

C

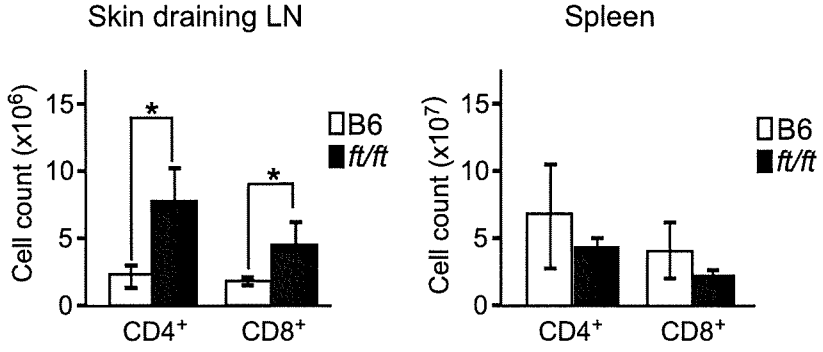

Figure 4
Moniaga et al.

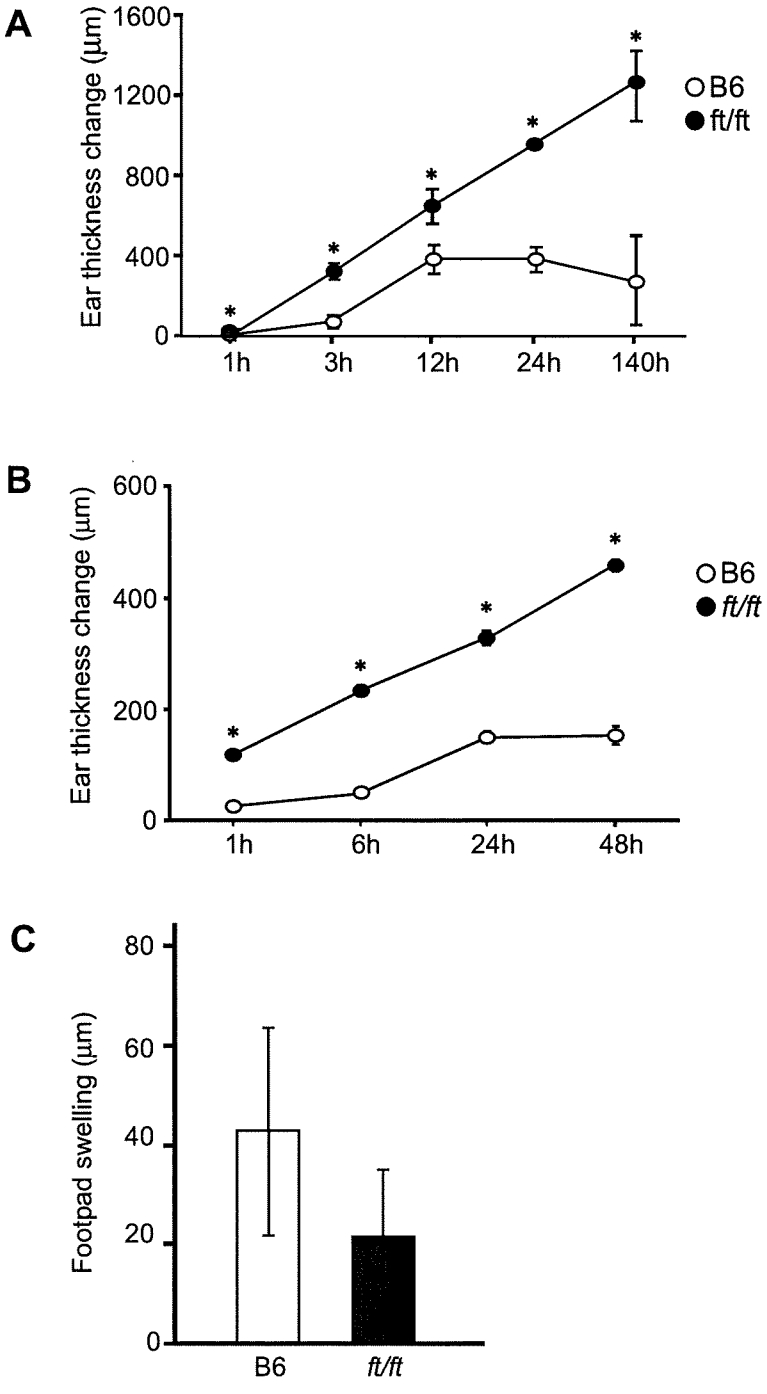

Figure 5
Moniaga et al.

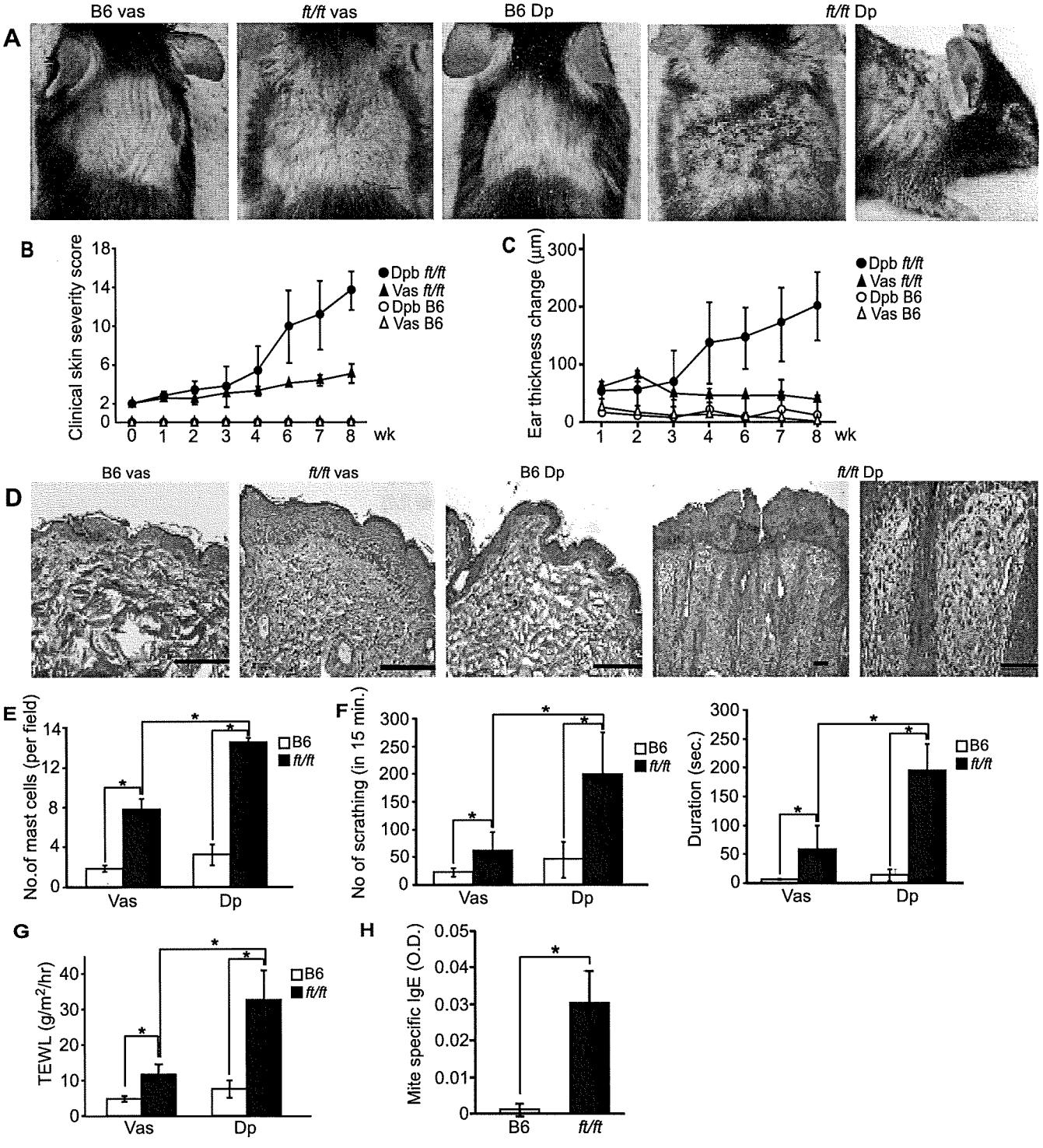

The mandatory role of IL-10-producing and OX40L-expresssing mature Langerhans cells in local UVB-induced immunosuppression

Running title: Langerhans cells and UVB-induced immunosuppression

Ryutaro Yoshiki*, Kenji Kabashima†, Jun-ichi Sakabe*, Kazunari Sugita*, Toshinori Bito*, Motonobu Nakamura*, Bernard Malissen‡, and Yoshiki Tokura*

* Department of Dermatology, University of Occupational and Environmental Health

† Department of Dermatology, Kyoto University

‡ Centre d'Immunologie de Marseille-Luminy, Institut National de la Santé et de la Recherche Médicale U631, Centre National de la Recherche Scientifique UMR6102, Université de la Méditerrannée

Phone/Fax: 81-93-691-7445/81-93-691-0907

e-mail: yockey@med.uoeh-u.ac.jp

Abstract

The mechanism underlying the local UVB-induced immunosuppression is a central issue to be clarified in photoimmunology. There have been reported a considerable number of cells and factors that participate in the sensitization phase-dependent suppression, including Langerhans cells (LCs), regulatory T cells (Tregs), and IL-10, and tumor necrosis factor-α. The recent important finding that LC-depleted mice rather exhibit enhanced contact hypersensitivity (CHS) responses urged us to re-evaluate the role of LCs along with dermal dendritic cells (dDCs) in the mechanism of UVB-induced immunosuppression. We studied the surface expression of OX40 ligand (OX40L) and the intracellular expression of IL-10 in LCs and dDCs from UVB (300 mJ/cm^2)-irradiated skin of BALB/c mice and those migrating to the regional lymph nodes from UVB-irradiated, hapten-painted mice. In epidermal and dermal cell suspensions prepared from the UVB-irradiated skin, LCs expressed OX40L as well as CD86 and produced IL-10 at a higher level than Langerin- dDCs. The UVB-induced immunosuppression was attenuated by the administration of IL-10-neutralizing or OX40L-blocking antibody. In mice whose UVB-irradiated, hapten-painted skin was dissected one day after hapten application, the CHS response was restored, because this treatment allowed dDCs but not LCs to migrate to the draining lymph nodes. Moreover, LC-depleted mice by using Langerin-diphtheria toxin receptor (DTR)-knocked-in mice showed impaired UVB-induced immunosuppression. These results suggest that

IL-10-producing and OX40L-expressing LCs in the UVB-exposed skin are mandatory for the induction of antigen-specific Tregs.

Introduction

Ultraviolet radiation (UV) is one of the significant environmental factors affecting humans or other animals. It is well known that UV, in particular the middle wave length range (290-320 nm, UVB), can be hazardous to human skin by acutely evoking sunburn and epidermal cell death and by chronically inducing skin cancers and skin aging (1-4). UVB radiation also exerts an immunomodulating effect on cutaneous contact hypersensitivity (CHS) by affecting various skin-constituent cells and factors (5). Preirradiation of sensitizing area with low-dose UVB suppresses the development of CHS to hapten in mice (6). In addition to the failure to generate hapten sensitization, mice develop tolerance, since animals treated in this way cannot be resensitized with the same hapten at a later time point. The UVB-induced immunosuppression appears to be hapten-specific, because the sensitization with other non-related haptens is not affected (6). Moreover, this hapten-specific immunosuppression can be transferable, as an injection of lymph node cells or splenocytes from UVB-tolerized mice into naïve mice inhibits the sensitization with the relevant hapten in the recipients (7). It was once considered that the UVB-induced immunosuppression was mediated by hapten-specific suppressor T cells (5, 8, 9). Now, this suppressor T cell is renamed regulatory T cell (Treg) (10-12). Therefore, a suppressive signal that causes UVB-induced tolerance is hypothesized to exist in the draining lymph node (DLN) of UVB-irradiated skin, where Tregs are induced and suppress the generation or function of effector T cells. However,

it remains unclear how the suppressive signal is transmitted from the skin to the DLNs. On one hand, Tregs act in part through the induction of IL-10 production (13). On the other hand, IL-10 is a key cytokine to induce Tregs, and keratinocytes have been considered to be the source of IL-10. However, all the mechanisms underlying UVB-induced immunosuppression are not attributed to keratinocyte-derived IL-10, because human keratinocytes are incapable of producing IL-10 (14). More fundamentally, keratinocytes are unable to migrate to the DLN. Therefore, alternative cells with a migrating ability are likely responsible for mediation of suppressive signals.

Recent studies have revealed the involvement of OX40 (CD134) and its ligand (OX40L) in T cell-antigen-presenting cell (APC) interaction (15-18). OX40 is expressed on activated CD4+ T cells and on certain populations of CD8+ T cells (15-17, 19), while OX40L is expressed on APCs such as activated B cells (20), dendritic cells (DCs) (21, 22), microglia (23), and endothelial cells (24). Ligation of OX40L on human DCs enhances their maturation and production of cytokines (22) and blockade of OX40L during naïve T cell-DC interaction suppresses the development of IL-4-producing T cells (25). It is thus suggested that OX40 and OX40L play an important role in the interaction of DCs with T cells to induce, in particular, Th2 cells. Moreover, CD4+CD25+ Tregs express OX40 at a high level compared with CD4+CD25- T cells (26, 27). Considering that UVB-induced suppressor T cells were historically identified as Th2 cells (28), these findings provide an implication that OX40-OX40L interaction

participates in the development of UVB-mediated CD4+CD25+ Tregs.

Langerhans cells (LCs) are capable of migrating from the epidermis into the DLNs on sensitization (29). Several investigator groups have suggested that LCs are responsible for induction of Tregs (30, 31), but the mechanism underlying the Treg induction by DCs in the UVB-irradiated skin remains unclear in major parts. Recent immunological studies have demonstrated that there are dermal DCs (dDCs), including Langerin+ dDCs and Langerin- dDCs in the murine skin (32-36). This raises the possibility that not only LCs but also dDCs have an ability to induce Tregs by UVB irradiation of the skin.

Here, we demonstrate that UVB irradiation of the skin leads to IL-10 production and OX40L expression by LCs. Our study using Langerin diphtheria-toxin-receptor (DTR)-knocked-in mice shows that the IL-10-producing and OX40L-expressing LCs plays a mandatory role for the induction of Tregs.

Materials and Methods

Animals and reagents

Six-10 week-old BALB/c female mice were purchased from Kyudo Co., Ltd. Mice were maintained on a 12-hour light/dark cycle under specific pathogen-free conditions. Langerin-DTR-knocked-in mice was generated (37). To deplete Langerin+ cells, mice were injected intraperitoneally with DT (100 ng each; Sigma, St. Louis, Missouri). Protocols were approved by the Institutional Animal Care and Use Committee of the University of Occupational and Environmental Health.

Contact hypersensitivity

Mice were sensitized with DNFB by applying 50 μl of 0.5% dinitrofluorobenzene (DNFB) in acetone /olive oil (4:1) to the shaved abdomen on day 0. On day 5, 20 μl of 0.2% DNFB was applied to both ears for elicitation. Ear swelling was measured with a micrometer 24 hours after elicitation.

UVB irradiation

The shaved abdomen was exposed to UV with a bank of four UVB lamps (Toshiba FL 20S, Toshiba Medical Supply, Tokyo) (5, 8, 9) that emit most of their energy within the UVB range (290-320 nm), with an emission peak at 313 nm. The irradiance was measured with an UVR-305/365 digital radiometer (Tokyo Kogaku Kikai KK, Tokyo, Japan). Mice were exposed to 300 mJ/cm^2 UV on the shaved abdomen on day -2 before sensitization (day 0). Although BALB/c mice are usually not very much susceptible to

UVB, we found that single exposure of BALB/c mice to UVB at 300 mJ/cm^2 induces UVB immunosuppression with an elevated percentage of Foxp3+ CD25+ cells in the DLN cells. Since single irradiation of the skin to UVB and following FITC paining are convenient for the study of DC migration to the DLN, we used this protocol and strain of mice in this study. The ears of mice were protected from radiation with opaque foil.

Culture medium

RPMI-1640 (Gibco BRL Life Technology Inc., Grand Island, NY) was supplemented with 10% heat-inactivated FCS, 2mM L-glutamine, 5 x 10^{-5} M 2-mercaptoethanol, 10^{-5} M sodium pyruvate, 25 mM HEPES, 1% non-essential amino acids, 100 units/ml penicillin, and 100 μg/ml streptomycin (all from Gibco).

Preparation of whole skin suspensions

Skin sheets from mouse abdomen were floated in 0.2% of trypsin in PBS (pH 7.4; Sigma) for 30 minutes at 37 °C as described previously (38). The epidermis was separated from the dermis with forceps in PBS supplemented with 10% fetal calf serum (FCS). Both epidermis and dermis were minced and incubated for 1 hour at 37°C in PBS with collagenase II (Sigma). The obtained cells were filtered through 40 μm filter.

Flow cytometry

Cells were immunostained with various combinations of fluorescence-conjugated mAbs and analyzed with FACSCanto flow cytometer (BD Biosciences, San Diego, CA) and FlowJo software (Tree star Inc., Ashland, Ohio). The expression of cell surface or

intracellular molecules and intracytoplasmic cytokines were analyzed using the following antibodies: Alexa Fluor 488-conjugated anti-epithelial cell adhesion molecule (EpCAM; Biolegend, San Diego, CA); PE-conjugated anti-OX40 ligand (OX40L), anti-CD86, anti-RANK, anti-rat IgG; APC-conjugated anti-MHC class II antibody; biotin-conjugated anti-mouse CD207 (Langerin), anti-IL-10 antibody, and anti-rat IgG; and PE-Cy7-conjugated streptoavidine (eBioscience, San Diego, CA). Intracytoplasmic IL-10 and Langerin was detected in permeabilizaed cell suspensions using BD cytofix/cytoperm Plus Kit (BD Bioscience).

Cutaneous DC migration into DLNs

Mice were painted on the clipped abdomen with 200 μl of 2% FITC (Sigma), and axillar and inguinal lymph nodes were taken 24 hours later. Single cell suspensions were prepared and subjected to flow cytometric analysis.

Apoptosis analysis

Twenty four hours after UVB irradiation (300 mJ/cm^2), whole skin suspensions were stained with APC Cy-7-conjugated anti-MHC class II, or PE-conjugated EpCAM and FITC-conjugated CD103 (BD Bioscience) for 30 min and stained with Alexa Flour 647-conjugated Annexin V (Invitrogen, Carlsbad, CA) and 7-AAD (BD Bioscience), according to the manufacture's protocol. Apoptosis in keratinocytes or DCs was analyzed by FACSCanto using FlowJo software as previously described (39).

In vitro promotion of LC IL-10 production by RANKL and its blockade with with neutralizing antibody against RANK

Freshly isolated epidermal cell suspensions (5 x 10^5/well) were cultured with or without 1 μg/ml of recombinant RANKL (R&D Systems, Minneapolis, MN) for 24 hour. For RANK neutralizing assay, 1 μg/ml of anti-RANK antibody (R&D Systems, Minneapolis, MN) was added to the culture 3 hours before the addition of recombinant RANKL. Intracellular IL-10 of LCs was measured by FACS.

***In vivo* neutralization of IL-10 and blocking of OX40L**

Mice received intraperitoneal injections of 25 μg anti-mouse IL-10 antibody (R&D Systems, Minneapolis, MN) or 10 μg anti-mouse OX40L antibody (Biolegend) for four consecutive days (on days 1 to 4) after UVB irradiation (on day -2) and DNFB sensitization (on day 0). They were challenged with DNFB on day 5, and the ear swelling responses were measured. For control, mice received the same volume of PBS and sensitized and challenged with DNFB.

Statistical analysis

All data were statistically analyzed using Student's *t*-test. *P* value of less than 0.05 was considered to be significant. Bar graphs were presented as mean ±SD of the mean value.

Results

Langerin+ dDCs are decreased in number and become apoptotic in UVB-irradiated skin.

It is a long-history concept that LCs play a critical role for CHS, as they serve as APCs and migrate to the draining lymph nodes (40). However, recent immunological studies have demonstrated that not only LCs but also Langerin+ dDCs and Langerin- dDCs exist in the skin and may differentially function as APCs. We first investigated the numerical change of LCs, Langerin+ dDCs, and Langerin- dDCs in the UVB-irradiated skin. Whole skin suspensions were prepared from the UVB-irradiated and non-irradiated skin as control 24 hours after UVB exposure and analyzed by flow cytometry. Using anti-MHC class II, anti-CD11c, anti-Langerin (CD207) and EpCAM antibodies, skin-resident DCs were clearly sorted out of the suspensions (Fig. 1A, B). As assessed by the percentage analysis, the populations of LCs (Langerin+ EpCAM+) and Langerin- dDCs (Langerin- EpCAM-) showed no substantial change after UVB irradiation (Fig. 1C *vs* D), although UVB-irradiated skin-derived DCs had a slightly broader MHC class II expression (Fig. 1B). However, the percentage of Langerin+ dDCs was dramatically decreased in UVB-irradiated skin (Fig. 1C *vs* D). When the absolute number of each LC/DC subset per skin specimen was calculated, UVB irradiation reduced dramatically the number of Langerin+ dDCs and moderately that of LCs, and did not affect that of Langerin- dDCs (Fig. 1E), confirming the decreased

number of Langerin+ dDCs in the UVB-irradiated skin. We analyzed apoptosis of LCs and DCs in the UVB-irradiated mice. Six hours after UVB irradiation, we assessed apoptotic cells by flow cytometry and defined as Annexin V+ and 7-AAD- cells. Langerin+ dDCs and LCs became apoptotic after UVB irradiation (Fig. 1F). There was no selectivity for UVB-induced apoptosis in these two subsets, but when they were compared in the apoptotic cell percentage, Langerin+ DCs were more sensitive to UVB. In contrast to these cells, Langerin- DCs were resistant to UVB.

LCs but not Langerin+ dDCs migrate from UVB-irradiated skin to DLNs.

We examined the numbers and migration timings of LCs, Langerin+ dDC, and Langerin- dDCs in the DLNs after FITC application of UVB-irradiated or non-irradiated skin. UVB-irradiated (day -2) and non-irradiated control mice were painted with FITC (day 0). On days 1-4, single cell suspensions were prepared from the DLNs and stained with anti-CD11c, anti-EpCAM and anti-Langerin antibodies. By flow cytometry, LC subset (Langerin+ EpCAM+) and Langerin+ dDC subset (Langerin+ EpCAM-) of CD11c+ FITC+ cells were detected in the DLNs. LCs were gradually increased in number in both UVB-irradiated and non-irradiated groups (Fig. 2A). On the other hand, the number of Langerin+ dDCs peaked on day 3 in non-irradiated mice, but their number in UVB-irradiated mice was very low (Fig. 2B). The number of Langerin- dDCs in UVB-non-irradiated skin was increased until day 2 and gradually declined, while that in UVB-irradiated skin peaked on day 1 and rapidly decreased (Fig.